Interferometric Study of Creep Deformation and Some Structural Properties of Polypropylene Fiber at Three Different Temperatures

I. M. Fouda, K. A. EL-Farahaty, E. A. Seisa

Physics Department, Faculty of Science, Mansoura University, Mansoura, Egypt

Received 4 February 2007; accepted 8 March 2008
DOI 10.1002/app.28714
Published online 10 July 2008 in Wiley InterScience (www.interscience.wiley.com).

ABSTRACT: Influence of temperature on creep deformation for polypropylene PP fiber under a constant load was studied interferometrically. The automated multiple-beam Fizeau system in transmission was equipped with a mechanical creep device attached to a wedge interferometer. This system was used to determine the optical properties ($n^{\parallel}$, $n^{\perp}$, and Δn) of PP fiber during the creep process at constant loading with varying temperature. The creep compliance was drawn as a function of both time and temperature. An empirical formula was suggested to describe the creep compliance curves for PP fibers and the constants of this formula were determined. Two Kelvin elements combined in series were used to provide an accurate fit to the experimental compliance curves. The stress–strain curve via creep was studied to determine some mechanical parameter of PP fibers, Young's modulus E, yield stress σ_y, and yield strain ε_y. The optical orientation function $f(\theta)$, the dielectric constant d, the dielectric susceptibility χ, the surface reflectivity $\overline{R}$, and the average work per chain W' were also calculated. © 2008 Wiley Periodicals, Inc. J Appl Polym Sci 110: 761–768, 2008

Key words: interferometry; creep compliance; orientation; birefringence; reflectivity; polypropylene

INTRODUCTION

Time-dependent deformation of a material under sustained constant load is referred to as creep. If the load is large and the duration is long, failure (i.e., creep-rupture) will occur. Many materials display linear viscoelastic behavior over certain ranges of stress and strain, but are nonlinear over larger ranges of these variables. Linear viscoelastic behavior has been well documented and a number of constitutive equations have been presented.[1–3]

The study of optical anisotropy in polymer fibers plays an important role in the knowledge of the molecular arrangement within the fibers. It is well known that birefringence is one of the most sensitive indicators of the anisotropy in polymers fibers; the degree of macromolecular orientation.

Techniques based on optical birefringence were used to measure the degree of the molecular alignment in uniaxially oriented fibers.[4–11] The changes in the optical anisotropy and orientation for polymer fibers by creep extension can be evaluated interferometrically by the measurement of refractive indices and birefringence of these fibers. Synthetic fibers in the drawn or extended state show considerable optical and mechanical anisotropy.[12–17] The automated multiple-beam Fizeau fringes system is an accurate and nondestructive technique in the field of fiber research.[18,19] Its is used to determine the mean refractive indices and birefringence at different processing.

In this work the influence of temperature on creep deformation based on optical properties of PP fiber were studied. The study investigated opto-mechanical behavior of fibers subjected to sustained constant load in time range of 0–230 min. Investigations were carried out via an automatic multiple-beam Fizeau interferometry with mechanical creep device[20] connected to a wedge interferometer. Measurements were carried out at three different temperatures (23, 30, and 40°C).

THEORETICAL CONSIDERATION

Creep

The creep results can be well represented by compliance $J(t)$, which is a measure of the strain per unit of applied stress.[2,3]

$$J(t) = \varepsilon(t)/\sigma_0 \tag{1}$$

where σ_0 is the constant static engineering stress applied to the specimen during creep and $\varepsilon(t)$ is the

Correspondence to: E. A. Seisa (seisa@mans.edu.eg).

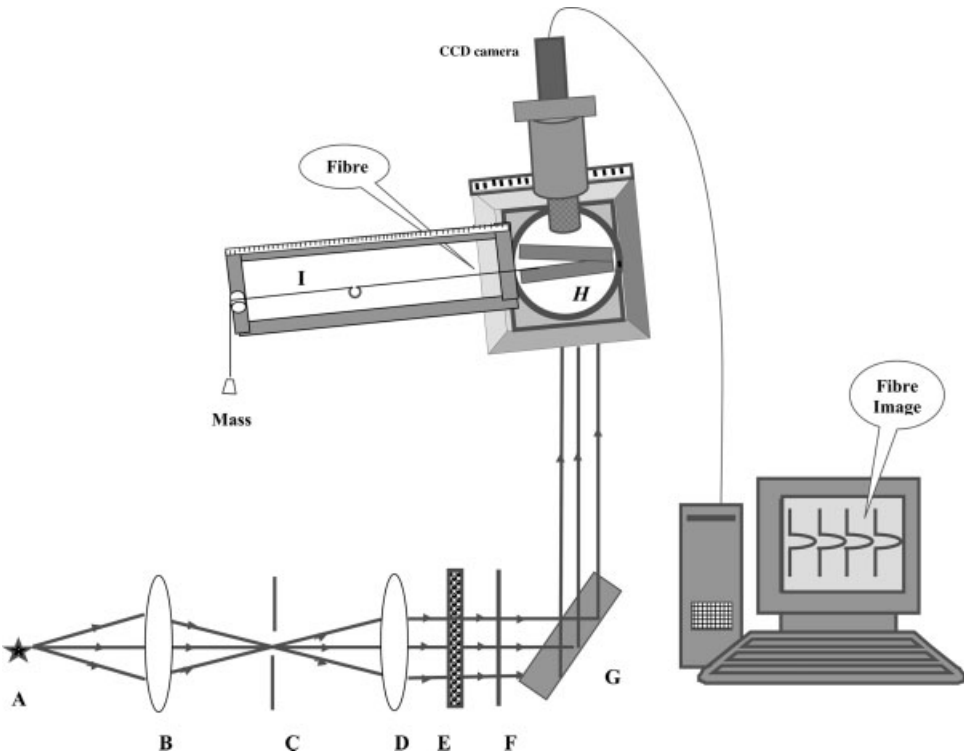

Figure 1 Schematic diagram of the mechanical creep device attached to automated optical system for producing multiple beams Fizeau fringe in transmission. (A) Mercury lamp, (B) condenser lens, (C) iris diaphragm, (D) collimating lens, (E) polarizer, (F) monochromatic filter, (G) reflector, (H) wedge interferometer, and (I) stretched string.

engineering strain. In the linear viscoelastic regime, $J(t)$ is only a function of temperature and time. We have determined the time dependence of creep compliance $J(t)$ as a function of time for PP fibers at three different temperatures.

Refractive indices ($n^{\parallel}$, $n^{\perp}$) and birefringence Δn

Multiple-beam Fizeau system in transmission was used for measuring the mean refractive indices ($n^{\parallel}$, $n^{\perp}$) and birefringence (Δn) for undrawn PP fibers under a constant load at different temperatures.[19]

The optical and mechanical orientation functions

The optical orientation function $f_{\Delta}(\theta)$ was calculated using Hermans[21] and Ward[22,23] equations

$$f_{\Delta}(\theta) = \Delta n/\Delta n_{\max} \tag{2}$$

where ($\Delta n_{\max}$ is the maximum birefringence of a fully oriented fiber. Its value has been previously[21] determined to be 0.045 for PP fiber. Hermans represented the orientation function $f(\theta)$ by a series of spherical harmonics (Fourier series)[21,24]

$$f(\theta) = \sum_{n=0}^{\infty}\left(n+\frac{1}{2}\right)\langle f_n\rangle f_n(\theta) \tag{3}$$

A sample with orientation function may be considered to consist of perfectly aligned molecules of the mass fraction (f and randomly oriented molecules of the mass fractio n $(1-f)$.

The deformations of a semi crystalline polymer can be described by the Kratky model.[24] On the basis of this model, Zbinden[25] has derived an expression for the distribution of function with draw ratios. From this expression the orientation function f can be calculated as

$$f = 1 - \frac{3}{2}\left[1 - \frac{D^3}{D^3-1} + \frac{D^3}{(D^3-1)^{3/2}}\cos^{-1}\left(\frac{1}{D^{3/2}}\right)\right] \tag{4}$$

where D is the draw ratio.

Determination of the dielectric constant and dielectric susceptibility

The dielectric constant is given by the following relation[26]

$$d = \frac{1+2(4\pi N_m\bar{\alpha}/3)}{1-(4\pi N_m\bar{\alpha}/3)} \tag{5}$$

where $\bar{\alpha}$ is the mean polarizability of a monomer unit and N_m is the number of molecules per unit volume. The dielectric susceptibility χ is related to the dielectric constant d by the following equation

$$\chi = \frac{d-1}{4\pi} \tag{6}$$

Calculation of the surface reflectivity

The surface reflectivity, $\overline{R}$ of a polymer for normal light can be estimated from Fresnel equation[27]

$$\overline{R} = \left(\frac{n-1}{\bar{n}+1}\right)^2 \times 100 \tag{7}$$

where $\bar{n}$ is the mean refractive index.

The average work per chain

The average work per chain W' for a collection of chains will depend on the distribution of chain-end distances, and was obtained by the following equation[28]

$$W' = \frac{3KT}{2}\left[\frac{1}{3}(D^2 - D^{-1}) + (D^{-1} - 1)\right] \tag{8}$$

where K is the Boltzman constant and T is the absolute temperature.

EXPERIMENTAL

The monomer Polypropylene $(CH_2{=}CH{-}CH_3)_n$ is related to ethylene and like ethylene possesses a double covalent bond, which may split to allow addition polymerization to take place due to stretching.[29]

The cross section of the tested PP fibers was observed using high power optical microscope to be perfectly circular with a diameter of 71.15 μm.

Three samples of undrawn PP fibers (draw ratio = 1) were investigated at the temperature 23, 30, and 40°C, respectively. The initial fiber length was 13 cm and each sample was elongated for time range of 0–230 min under constant load of 13 g. The refractive indices of the immersion liquids used were 1.501, 1.486, and 1.466 for the temperatures 23, 30, and 40°C, respectively.

Figure 1 shows the optical system, which was used to produce multiple-beam Fizeau fringes in transmission and a computer with a CCD camera attached. A parallel beam of plane polarized monochromatic light of wavelength 546.1 nm was used to illuminate the wedge interferometer H placed on a microscope stage. The fiber was immersed in a liquid and orientated in perpendicular to the edge of the wedge. Straight line fringes parallel to the edge of the wedge are formed in the liquid region. The amount, shape, and direction of fringe shift crossing the fiber depends on the refractive index of the liquid n_L, the relative refractive indices of the fiber, the used wavelength and the stage of polarization of monochromatic light.

The variation of the interferometry patterns on the CCD camera were captured during creep process. The obtained microinterferograms were used to determine the mean refractive indices and mean birefringence of PP fibers at each value of creep strain under constant load. The values were determined for three different temperatures 23, 30, and 40°C, which were allowed by air condition for all the environment of laboratory.

The study of creep was conducted under conditions for stress σ = constant and the strain ε measured as a function of the time. The experimental results and discussion obtained for PP fibers are given in the following section.

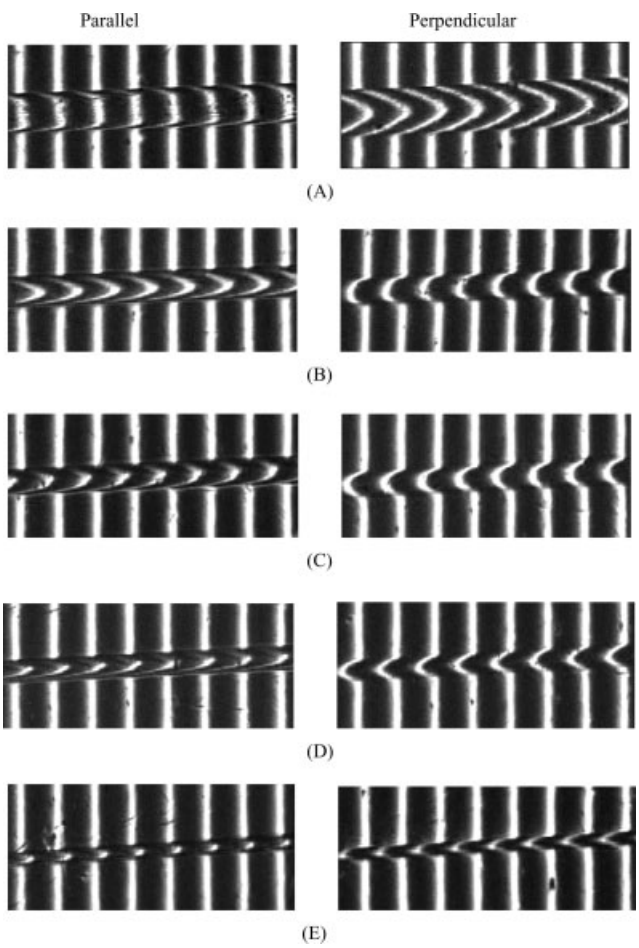

Figure 2 (A–E) Microinterferograms of multiple-beam Fizeau fringes in transmission for light vibrating parallel and perpendicular to fiber axis at temperature 30°C at a constant applied load (m = 13 g). The creep extensions for the interferograms are (A) 0%, (B) 84.62%, (C) 153.58%, (D) 269.23%, and (E) 450%.

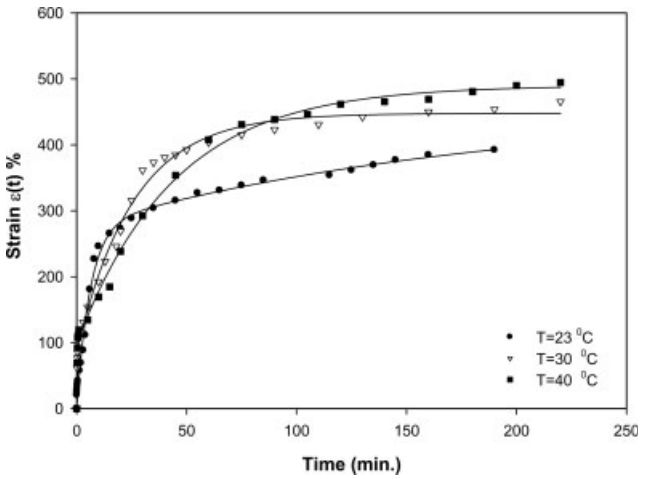

Figure 3 Creep strains of PP fibers as a function of time under constant load for three different temperatures (23, 30, and 40°C).

RESULTS AND DISCUSSION

Figure 2(A–E) are microinterferograms of multiple-beam Fizeau fringes in transmission for light vibrating parallel and perpendicular to the axis of PP fibers under a constant applied load of 13 g at temperature 30°C. The creep strain for the interferograms A to E were 0, 84.62, 153.58, 269.23, and 450%, respectively. The refractive index of the immersion liquid was 1.486 at 30°C. The fringe shift changes in the microinterferograms identifies differences in optical path variations due to increasing creep strain. It also shows the appearance of different shifts at different state of stretching (Creep). It can be seen that, there is a gradual decrease in fibers diameter and changes in the fringe shifts.

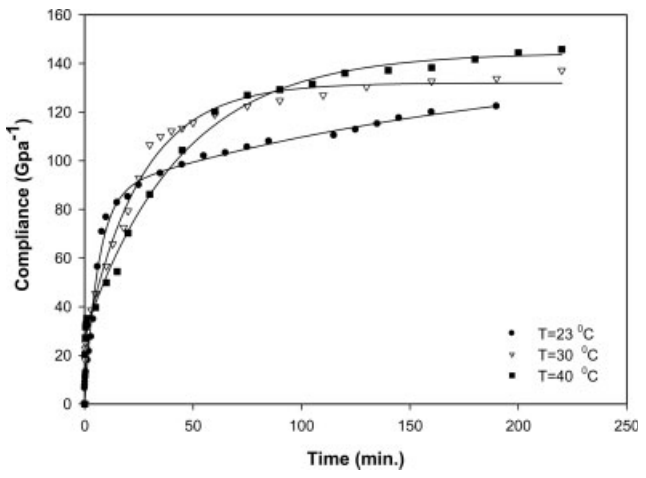

Figure 4 Creep compliance $J(t)$ as a function of time and temperature of PP fibers.

TABLE I
Values of the Constants in eq. (9) for PP Fibers

	Constants			
Temperature, T (°C)	a (Gpa^{-1})	b (s^{-1})	c (Gpa^{-1})	d (s^{-1})
23	85.9040	0.1625	57.0651	0.0054
30	25.5116	6.1370	106.4622	0.0387
40	29.0121	7.4511	115.3894	0.0226

Experimental description of the creep behavior of PP fibers

Polymeric materials, including fibers, show creep under static loading conditions. In polymers such as PP fiber, creep can be very extensive, both for nonoriented material as well as for highly oriented fibers. Figure 3 shows the creep strain for PP fibers as a function of time under constant load for three different temperatures. At loading times of 20, 35, and 60 min using different ambient temperatures, the creep strain rate initially decreased with the strain (primary creep) then it was constant with further increase of strain (secondary creep).

The resulting creep deformation of the material is characterized by creep compliance $J(t)$ as a function of time for PP fibers at different temperatures 23, 30, and 40°C (see Fig. 4). The initial part of these graphs up to loading time 5 min appears to be independent of temperature. In this region the process is linear. At long loading time, the compliance depends on temperature and the creep process is nonlinear.

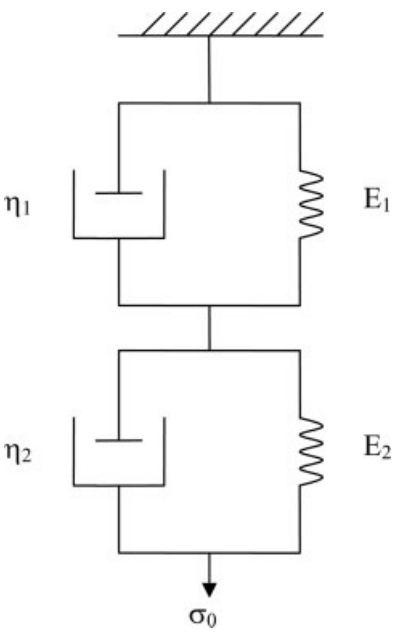

Figure 5 Two Kelvin model in series.

TABLE II
Values of the Constants in eq. (10) for PP Fibers

Temperature, T (°C)	Constants					
	E_1 (Gpa)	τ_1 (s)	η_1 (Gpa s)	E_2 (Gpa)	τ_2 (s)	η_2 (Gpa s)
23	0.0116	6.1538	0.0716	0.0175	185.1852	3.2452
30	0.0392	0.1629	0.0064	0.0094	25.8398	0.2427
40	0.0345	0.1342	0.0046	0.0087	44.2478	0.3835

Creep analysis

The two Kelvin model in series

A good description of the experimental values of the creep compliance $J(t)$ for PP fibers was obtained from our suggested empirical relation

$$J(t) = a(1 - e^{-bt}) + c(1 - e^{-dt}) \quad (9)$$

where a, b, c, and d were empirically determined and listed in Table I.

Figure 5 illustrates the combination of the two Kelvin elements in series (the elastic element represented by a spring and the viscous element represented by a dashpot). It is the simplest model that exhibits all the essential features of viscoelasticity, on the application of a stress σ, the model suggests an elastic deformation, followed by creep as shown in Figures 3 and 4.

The model represented in Figure 5 shows creep compliance curves similar to those of PP fibers in Figure 4. It would elongate with time under a constant load according to the following equation, which was given by Ward and Hadley[2]

$$J(t) = \frac{1}{E_1}(1 - e^{-t/\tau_1}) + \frac{1}{E_2}(1 - e^{-t/\tau_2}) \quad (10)$$

where E_1, E_2 are the spring moduli, $\tau_1 = \eta_1/E_1$, $\tau_2 = \eta_2/E_2$ are the retardation times, η_1 and η_2 the dashpot viscosities. The values of E_1, E_2, τ_1, τ_2, η_1, and η_2 were determined from the corresponding constants a, b, c, and d given by eq. (9). The results were tabulated in Table II.

The two Kelvin model in series, when a constant load is applied, the initial elongation comes from the springs with moduli E_1 and E_2. Later elongation comes from the movement of dashpots with viscosities η_1 and η_2. The total elongation J of the model is the sum of the individual elongation of the two parts. The change of the elongation with time was given by eq. (10).

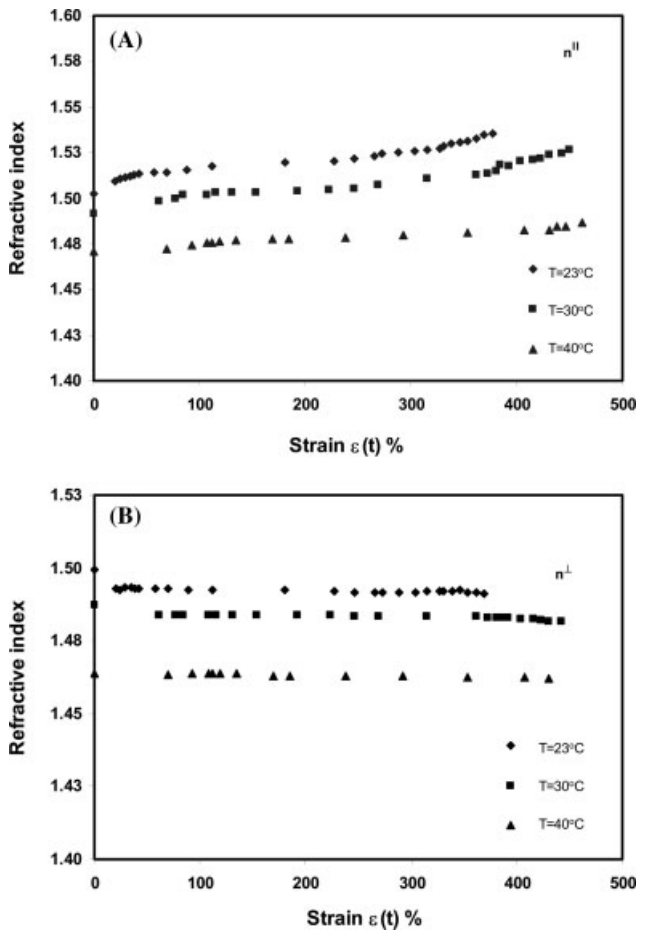

Figure 6 (A) Variation of the mean refractive index $n^{\parallel}$ with the creep strain ε(t)% at different temperatures. (B) Variation of the mean refractive index $n^{\perp}$ with the creep strain ε(t)% at different temperatures.

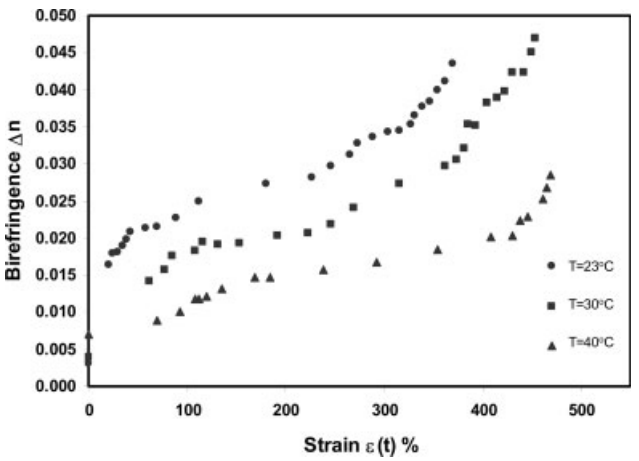

Figure 7 Variation of mean birefringence Δn with the creep strain ε(t)% at different temperatures.

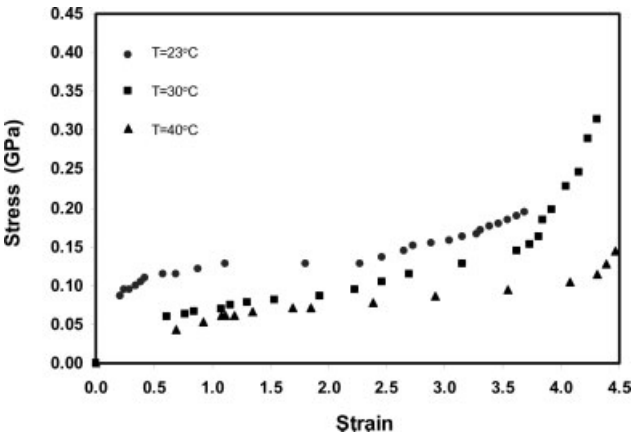

Figure 8 Stress–strain curves of PP fibers under constant load.

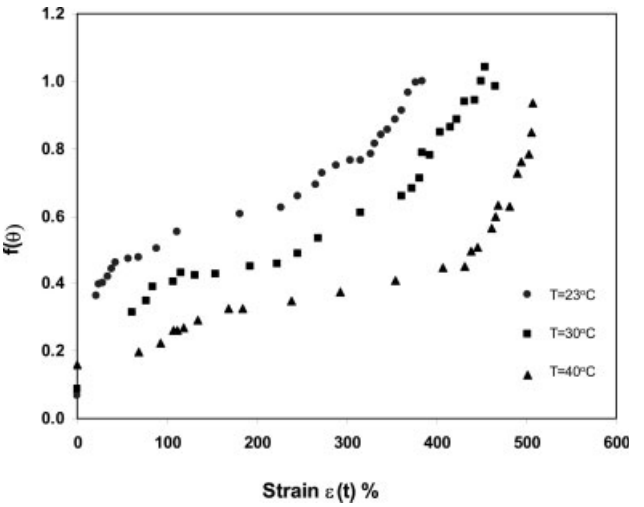

Figure 9 The relationships among the optical orientation function $f(\theta)$ and the creep strain $\varepsilon(t)\%$.

Influence of the creep strain on the refractive indices ($n^{\parallel}$, $n^{\perp}$) and birefringence Δn

The experimental values of the mean refractive indices and mean birefringence of PP fibers at each value of creep strain at constant loading for various temperatures were determined using optical equations, which are discussed elsewhere.[17]

Figure 6(A, B) shows the variation of mean refractive indices ($n^{\parallel}$, $n^{\perp}$) with creep strain, $\varepsilon(t)\%$ for three different temperatures. It was observed that the creep strain increased the refractive index $n^{\parallel}$, but decreased the refractive index of $n^{\perp}$. The changes in $n^{\parallel}$ were greater and more obvious than that of $n^{\perp}$. This behavior means that during extension the fiber chains become oriented in the direction of extension (parallel to the fiber axis). For a given creep strain the values of both the refractive indices $n^{\parallel}$, $n^{\perp}$ decrease at elevated temperatures. The variation of mean birefringence Δn with creep strain $\varepsilon(t)\%$ at different temperatures was shown in Figure 7. Its clear that, the mean birefringence Δn increases with increasing creep strain $\varepsilon(t)\%$. The mean birefringence decreased as the temperature increased, this means that the fibers material becomes less oriented.

Influence of the creep strain on some parameters

The stress–strain curves for PP fibers at different temperatures 23, 30, and 40°C were shown in Figure 8. From these curves, the values of Young's modulus E, yield stress σ_y, and yield strain ε_y for PP fibers were determined at different temperatures and tabulated in Table III. So it is found that, the values of Young's modulus and yield stress decrease and the yield strain increases with increasing temperatures.

TABLE III
Yield Stress σ_y, Yield Strain ε_y and Young's modulus E for PP Fiber at Various Temperatures

Temperature, T (°C)	Yield stress, σ_y (Gpa)	Yield strain, ε_y	Young's modulus, E (Gpa)
23	0.118	0.27	0.437
30	0.068	0.62	0.110
40	0.060	0.95	0.063

The optical orientation function $f(\theta)$ for PP fibers was calculated from eq. (2) at different temperatures. The relationship between the optical orientation function $f(\theta)$ and creep strain $\varepsilon(t)\%$ was shown in Figure 9. The mechanical orientation function f and its dependence on the creep strain $\varepsilon(t)\%$ is given in Figure 10.

The dielectric constant d and the dielectric susceptibility χ increase with creep strain of PP fibers under different temperatures and represented in Figures 11 and 12, respectively.

The values obtained for the surface reflectivity $\overline{R}$ was slightly increased with increasing of the creep

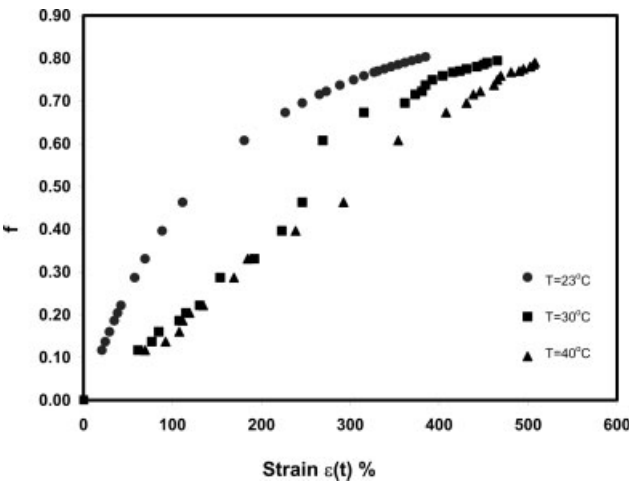

Figure 10 The dependence of the mechanical orientation function for the creep strain $\varepsilon(t)\%$.

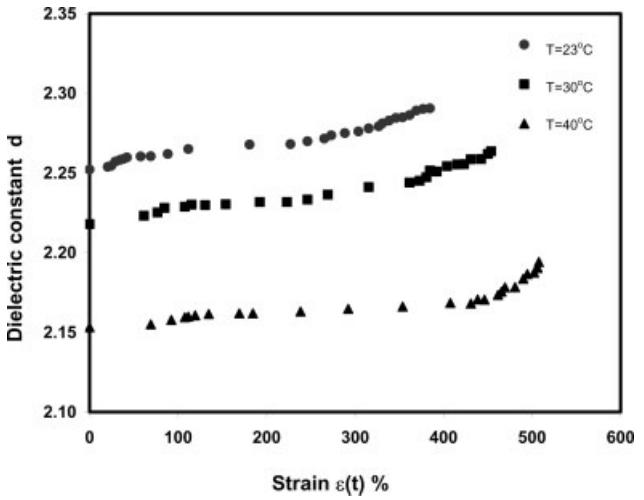

Figure 11 The dielectric constant d as function of the creep strain $\varepsilon(t)\%$.

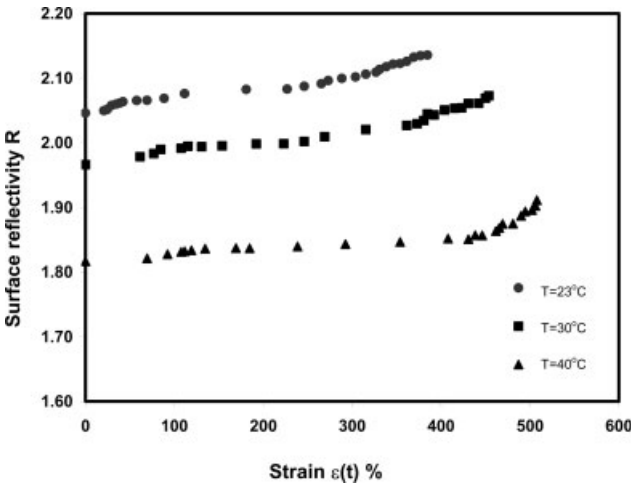

Figure 13 The surface reflectivity $\overline{R}$ increased with the increase of creep strain $\varepsilon(t)\%$.

strain as shown in Figure 13. Figure 14 shows the increasing of average work per chain W' with increasing the creep strain.

The behavior of polymeric material, when subjected to stress, varies considerably from one material to another. The structure of the polymer has a considerable effect upon the properties of the material. Birefringence and relaxation behavior of PP fibers were due to gradual transition from the rubber state to glass state. This probably results from the motions of segments within the chain backbone.

CONCLUSIONS

From the earlier measurements and calculations the following conclusions are drawn:

1. The creep compliance for PP fibers at constant sustained load fitted well with the suggested empirical formula, and the two Kelvin model in series was consistent with our empirical fitting formula (9).
2. The mean birefringence of PP fibers increases with the creep strain, so upon increasing the temperature, the orientation becomes relatively small.
3. Decreasing the value of Young's modulus with increasing creep temperature is attributed to the fact that resistance of the fiber material to the creep deformation becomes low at higher temperature.
4. The orientation function given by the two techniques (optical and mechanical) lead to increase as the strain increases. These techniques are suitable for the determination of molecular orientation parameters.
5. The obtained principal optical parameters are suitable for evaluating the dielectric constant,

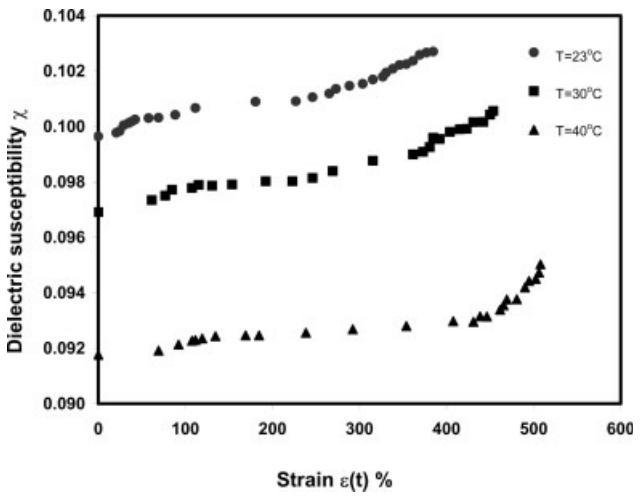

Figure 12 The dielectric susceptibility χ as function of the creep strain $\varepsilon(t)\%$.

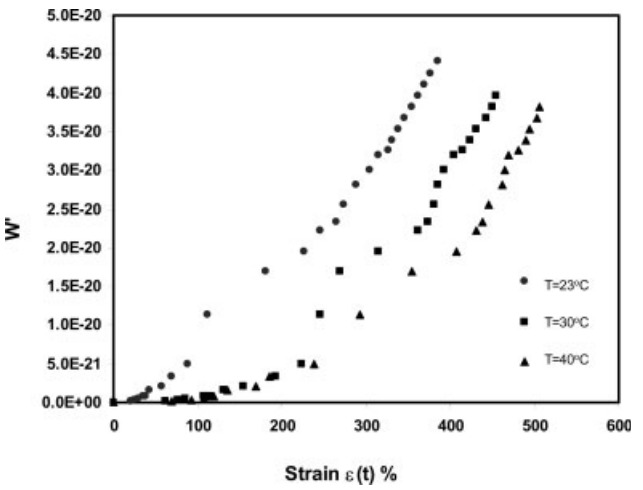

Figure 14 The average work per chain W' as a function of the creep strain $\varepsilon(t)\%$.

the dielectric susceptibility and surface reflectivity in PP fibers.

6. There are some new physical structural changes in the fiber due to creep strain under different conditions as indicated by the values of d, χ, $\overline{R}$, and W'.
7. The microinterferograms clearly identify difference in optical path variations due to the influence of creep and different temperatures.

From the earlier results and considerations, we concluded that the practical importance of this measurement provides acceptable results for the creep and optical parameter changes for PP fibers.

References

1. Findley, W. N. SPE J 1960, 16, 57.
2. Ward, I. M.; Hadley, D. W. An Introduction to the Mechanical Properties of Solid Polymer; Wiley: New York, 1993; p 58.
3. Sperling, I. H. Introduction to Physical Polymer Science, 4th ed.; Wiley: New York, 2006; p 507.
4. Nobbs, J. H.; Bower, D. I.; Ward, I. M. Polymer 1976, 17, 2.
5. Nobbs, J. H.; Bower, D. I.; Ward, I. M. Polymer 1978, 100, 19.
6. Bower, D. I.; Ward, I. M. Polymer 1982, 23, 645.
7. Neil, M. A.; Duckett, R. A.; Ward, I. M. Polymer 1988, 25, 54.
8. Samules, J. R. Structural Polymer Properties; Wiley: New York, 1974; p 50, 54, 63, 219.
9. Fouda, I. M. J Appl Polym Sci 1999, 73, 819.
10. Fouda, I. M. Polym Test 2002, 21, 3.
11. Treloar, L. R. G. The Physics of Rubber Elasticity; Oxford University Press: London, 1975; p 203.
12. El-Farahaty, K. A. J Appl Polym Sci 1986, 7, 621.
13. Hamza, A. A.; Fouda, I. M.; Sokkar, T. Z. N.; Shahin, M. M.; Seisa, E. A. Polym Test 1992, 11, 297.
14. Hamza, A. A.; Fouda, I. M.; Kabeel, M. A.; Seisa, E. A.; El-Sharkawy, F. M. Polym Test 1997, 16, 303.
15. Hamza, A. A.; Fouda, I. M.; Kabeel, M. A.; Seisa, E. A.; El-Sharkawy, F. M. J Appl Polym Sci 1998, 76, 1957.
16. Fouda, I. M.; El-Tonsy, M. M. Polymer Plastic Technology and Engineering; 2006, 45, 223.
17. Barakat, N.; Hamza, A. A.; Interferometry of Fibrous Materials; Hilger: UK, 1990.
18. Hamza, A. A.; Sokkar, T. Z. N.; Mabrouk, M. A.; EL-Morsy, M. A. J Appl Polym Sci 2000, 77, 3099.
19. Hamza, A. A.; Sokkar, T. Z. N.; EL-Farahaty, K. A.; EL-Morsy, M. A.; EL-Dessouky, H. M. Optics Laser Technol 2005, 37, 532.
20. El-Farahaty, K. A. Polym Test 1996, 15, 163.
21. Hermans, P. H. Contribution to the Physics of Cellulose Fibres; North Holand, Amsterdam, 1949; [Ref. Gedde, U. P. W. Polymer Physics; Chapman & Hall: London, 1995; p 194.]
22. Ward, I. M. Proc Phys Soc London 1962, 80, 1176.
23. Ward, I. M. J Polym Sci: Polym Symp 1977, 53, 9.
24. Kratky, O.; Kolloid-Z 1933, 64, 401. [Ref. Ward, I. M. Structure and Properties of Oriented Polymers Applied Science; London, 1975; p 68.]
25. Zbinden, R. Infrared Spectroscopy of High Polymers; Academic Press: New York, 1964.
26. Born, M.; Wolf, E. Principle of Optics, 2nd ed. Pergamon Press: Oxford, 1964; p 87.
27. Hemsley, D. A. Applied Polymer Light Microscopy; Elsevier Science: London, 1989; p 88.
28. Williams, D. J Polym Sci and Engineering; Prentice-Hall: Engle Wood Cliffs, NJ, 1971; p 190.
29. Veron, B. J. Introduction to Engineering Material; Macmillan: London, 1975; p 183.